Paleoproterozoic snowball Earth: Extreme climatic and geochemical global change and its biological consequences

Joseph L. Kirschvink*†, Eric J. Gaidos‡, L. Elizabeth Bertani§, Nicholas J. Beukes¶, Jens Gutzmer¶, Linda N. Maepa*, and Rachel E. Steinberger§

*Division of Geological and Planetary Sciences, ‡Jet Propulsion Laboratory, and §Division of Biology, California Institute of Technology, Pasadena, CA 91125; and ¶Department of Geology, Rand Afrikaans University, Auckland Park 2006, Johannesburg, South Africa

Geological, geophysical, and geochemical data support a theory that Earth experienced several intervals of intense, global glaciation (''snowball Earth'' conditions) during Precambrian time. This snowball model predicts that postglacial, greenhouse-induced warming would lead to the deposition of banded iron formations and cap carbonates. Although global glaciation would have drastically curtailed biological productivity, melting of the oceanic ice would also have induced a cyanobacterial bloom, leading to an oxygen spike in the euphotic zone and to the oxidative precipitation of iron and manganese. A Paleoproterozoic snowball Earth at 2.4 Giga-annum before present (Ga) immediately precedes the Kalahari Manganese Field in southern Africa, suggesting that this rapid and massive change in global climate was responsible for its deposition. As large quantities of O_2 are needed to precipitate this Mn, photosystem II and oxygen radical protection mechanisms must have evolved before 2.4 Ga. This geochemical event may have triggered a compensatory evolutionary branching in the Fe/Mn superoxide dismutase enzyme, providing a Paleoproterozoic calibration point for studies of molecular evolution.

Two major intervals of glacial activity punctuate the first four billion years of Earth's history. The first occurred during the Paleoproterozoic at about 2.4 Ga, and the other during Neoproterozoic time between about 0.8 and 0.6 Ga (1, 2). Unlike Paleozoic and younger glaciations, these two Precambrian deposits are closely associated with tropical rather than polar paleolatitude indicators such as carbonate rocks, red beds, and evaporites (1, 2). These observations are supported by paleomagnetic results indicating that Neoproterozoic glaciogenic rocks occur within 5° of latitude of the equator (3–5), and two exposures of the Paleoproterozoic glaciation occur within ≈11° of the equator (6, 7).

Climate models predict severe consequences of such low-latitude glaciation: An ice-albedo feedback will drive a run-away glaciation (8) resulting in 500–1,500 m of global oceanic pack ice and average surface temperatures reaching −20 to −50°C (9, 10). The hydrological cycle and continental weathering shut down except for minor sublimation (11–13), curtailing photosynthesis and biological productivity. Sea level would initially fall. However, ablation could eventually move the ice in continental glaciers to the floating pack ice, returning sea level to normal. Continued volcanism and hydrothermal fluid circulation at mid-oceanic ridge spreading centers, in concert with the curtailment of oxygenic photosynthesis and the isolation of the oceans from the atmosphere, would produce a metalliferous, reducing ocean chemistry. The greenhouse effect of a buildup of atmospheric CO_2 from continental volcanism and the lack of a silicate weathering sink for CO_2 at low temperature would allow eventual escape from such an ''icehouse'' state (8, 14). Surface temperatures would rise until the removal of ice at the equator injects water vapor into the atmosphere and triggers rapid melting of the entire ocean. Hoffman *et al.* (10) estimated that

between 4 and 30 million years (My) would be required for this CO_2 buildup in Neoproterozoic time.

Kirschvink (14) noted that the extreme geochemical environments predicted by a snowball Earth model explain the Neoproterozoic banded iron formations (BIFs). Hoffman *et al.* (10) extended the model to account for the deposition and isotopic composition of postglacial cap carbonates. Tsikos and Moore (15) suggested that the glacial deposits and the unique manganese (Mn) deposits of the Paleoproterozoic Hotazel formation in South Africa may be causally related, but without providing a mechanism. We suggest that a global glaciation followed by a cyanobacterial bloom provides a simple explanation of the manganese formations and furthermore describes an extraordinary event in the geochemical history of the planet, one with potentially profound implications for the evolution of life.

Geologic Setting. Sedimentary and volcanic rocks of the Transvaal Supergroup of southern Africa preserve one of the world's most complete and least metamorphosed record of late Archean and Paleoproterozoic time (Fig. 1). Glacially derived sediments of the Makganyene Diamictite are overlain by up to 900 m of subaqueous pillow lavas of the Ongeluk Formation, part of the Hekpoort/Ongeluk flood basalt series (16). These glacial sediments and the volcanics are coeval, as the units interfinger with each other and small volcanic fragments are often present in the highest layers of the diamictite (6). The volcanics also have a few thin jaspilite beds (red, cryptocrystalline quartz with abundant iron oxide layers) between flows. This indicates that the oceans were not sealed completely from atmospheric O_2 until after their deposition. Paleomagnetic results from the Ongeluk lavas indicate that they (along with the interbedded glacial sediments) formed within the tropics at a paleolatitude of 11 ± 5° (6). BIFs of the ≈100-m-thick Hotazel formation are draped over the uppermost surface of the unweathered, undulating volcanic pillows. Initial sediments above this contact usually include 10–20 cm of a fine-grained, immature and unsorted volcaniclastic sandstone. After this is about a 0.5- to 1-m thick unit of jaspilitic iron formation, with occasional small glacially deposited drop stones and sandy layers. These drop stones may record the rapid deglaciation at the end of the snowball. Above this is an initial layer of BIF followed by up to 45 m of manganese-rich carbonate in three separate pulses. The oceans gradually returned to normal conditions with deposition of the conformably overlying Mooidraai Dolomite.

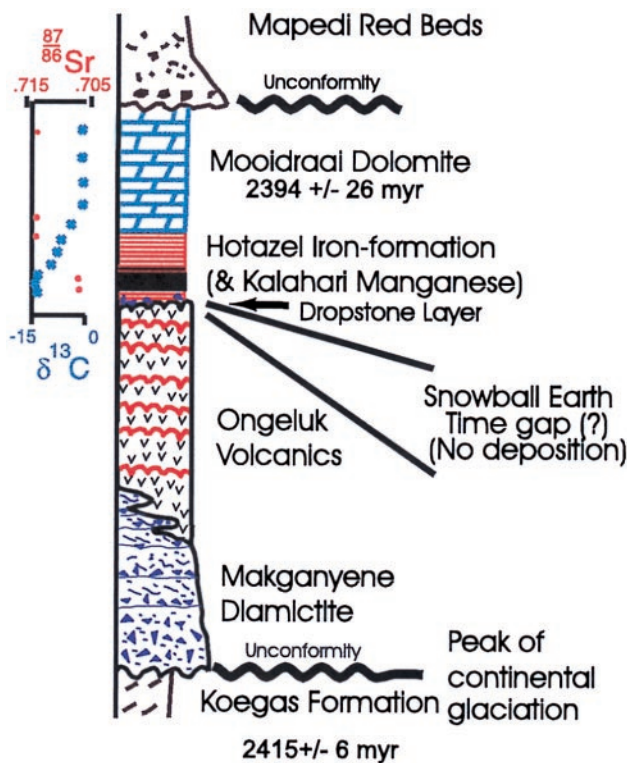The principal unconformity at the base of the Makganyene

---

Fig. 1. Stratigraphy of the Transvaal supergroup of southern Africa in the Griquitown West area, showing the relationships between the Mn-bearing units of the Hotazel Formation and the underlying volcanics and glacial sediments.

Fig. 2. Temporal distribution of major types of continental manganese (*Upper*) and iron ore (*Lower*) reserves of the world. Data are from ref. 23. Sedimentary Mn is extremely rare in pre-2.4-Ga rocks, reaching at most a 2% concentration in occasional carbonate beds.

diamictite has been bracketed recently by Pb/Pb ages of 2,415 ± 6 My on the Koegas formation and 2,394 ± 26 My on the Mooidraai dolomite, although younger ages of ≈2,200 My have been reported for the sequence (J.G. and N.J.B., unpublished work; refs. 17–19). Two lines of evidence imply that the major time gap in the sequence is represented by the contact between the Ongeluk lavas and the basal Hotazel formation (Fig. 1). First, many thick sequences of flood basalts form within an interval of one million years or less (20), which is short compared with inferred durations of ≈10 million years for a snowball event (10). Second, the drop stone layer at the base of the Hotazel formation suggests that that the glaciation lasted longer than Ongeluk volcanism, and hence this contact probably represents most of the time interval when the oceans were entombed under the ice cap. Manganese-rich layers within the Hotazel formation preserve over 13.5 billion metric tons of manganese ore [≈4 billion tons of Mn (Fig. 2)], making the Kalahari manganese field by far the world's largest land-based economic reserve of this element (21–23). Major deposits of Mn associated with BIFs occur only twice in the geological record, and both follow directly after inferred snowball Earth events in the Paleoproterozoic and Neoproterozoic (24–27). Except in areas in which the ore has been oxidized, most of the manganese is preserved as the mineral braunite (Mn^{+2} $Mn^{+3}_6SiO_{12}$) and finely intergrown Mn-rich carbonates, such as kutnahorite and Mn-calcite (21–23), whereas the underlying BIF is of the magnetite-hematite type. The Hotazel Formation appears to have been deposited below wave base, at maximum depths of about 200 m [i.e., continental shelves (23, 28)].

Manganese has a high oxidation potential ($E_0 = -1.29$ V with respect to the hydrogen standard), and the Kalahari manganese field seems to represent a transition in the oxidation state of Earth's sur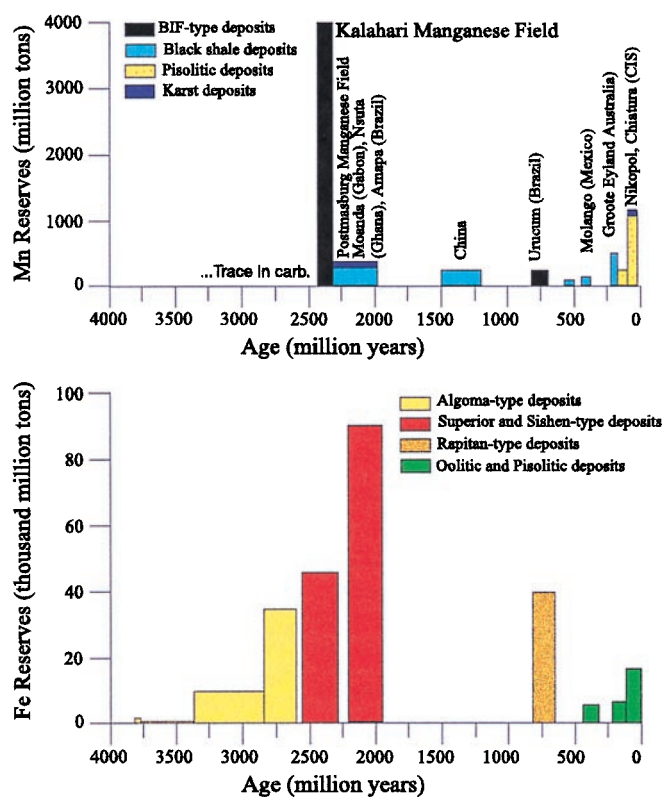face, which is in rough temporal agreement (J.G. and N.J.B., unpublished work; ref. 19) with oxygen constraints deduced from the study of Precambrian paleosols (29). Geochemical analyses of Mn concentrations in shallow-water carbonates demonstrate that deposition of the Kalahari manganese field represents a unique oxidation and Mn extraction event in the world oceans. Older Archean and earliest Proterozoic shallow-water carbonates typically contain up to a percent Mn whereas this metal is generally absent in carbonates younger than the Ongeluk/Hotazel/Mooidraai sequence (30–32). The redox state of the surface oceans apparently changed across this interval of time. This chemical difference is often clearly expressed during weathering, with the older carbonates forming a black Mn-rich surface rind, and under extreme conditions forming economically important Mn-karst deposits.

Snowball Biogeochemistry. During global glaciation, isolation of the ocean by a kilometer of ice and the absence of a hydrological cycle and carbonate formation would cause volcanically derived CO_2 to build up in the atmosphere, and hydrothermally derived Fe and Mn to accumulate in the ocean (14). At modern rates of activity, subaerial volcanism will increase atmospheric CO_2 levels at a rate of 9 mbar/My (1 bar = 100 kPa), and submarine volcanism will put the equivalent of 18 mbar/My into the entombed oceans (33). Standard stellar theory predicts a solar luminosity only 83% of the present value (34), and Caldeira and Kasting (8) calculate that a correspondingly large amount of atmospheric CO_2, about 1×10^{20} moles or 0.6 bar, would be required to raise average equatorial temperatures to above freezing and melt the ice. This amount of CO_2 will accumulate in about 70 My at present outgassing rates. Although Caldeira and Kasting (8) found that atmospheric CO_2 will become saturated and form polar clouds on Earth, it is now believed that

EVOLUTION

GEOLOGY

SPECIAL FEATURE

they will not attenuate the greenhouse effect of CO_2 (35). Thus, Earth would avoid the irreversible catastrophe suggested by Caldeira and Kasting. An additional greenhouse gas, such as SO_2 or dust, may have also been involved (36, 37). We assume that outgassing rates and hydrothermal circulation were more vigorous in the Paleoproterozoic by a degree proportional to the estimated higher heat flow (roughly a factor of two over present). Our estimate of the duration of a Paleoproterozoic snowball event is thus ≈35 My. The amount of Fe and Mn that accumulates in the ocean can be estimated by looking at the relative concentrations (with respect to CO_2) of hydrothermal vent fluids (38). We derive quantities of $1.5–15 \times 10^{18}$ mol of Fe and $0.8–2 \times 10^{18}$ mol of Mn. To the extent that subaerial volcanism scales with submarine hydrothermal circulation over geologic time, these estimates are independent of outgassing rates.

The accumulation of iron has direct consequences for marine biology and chemistry in the era immediately after the snowball event. Biological productivity in large areas of the modern oceans is limited by the availability of iron (39), trace amounts of which can stimulate phytoplankton blooms. For the postsnowball oceans, ferrous iron and most other essential nutrients for photosynthesis would be available in solution throughout the euphotic zone (38). Phosphorus would be liberated by the decay of organic matter in the snowball ocean, and magnesium (Mg) would be provided by aeolian debris from glacial erosion of Mg-rich continental rocks. Many of the low-latitude Precambrian glacial diamictites contain large concentrations of high-Mg carbonate (primary limestone and dolomite) (1, 2), and, after ablation of the continental ice sheets, winds would have distributed this glacial dust over Earth's entire surface. A snowball Earth would be followed by an oceanic bloom, perhaps by cyanobacteria of which fossil biomarkers have been found in older rocks of upper Archean age (40).

This photosynthetic bloom may have led directly to the precipitation of the Kalahari Manganese member of the Hotazel banded iron formation, as outlined schematically on Fig. 3. Oxygen released by the photosynthetic bloom should react with ferrous iron in solution to produce an initial layer of precipitated iron/manganese that would sink. However, the Mn^{+4} can be reduced by Fe^{+2} at lower depths, leaving iron as the initial precipitate, as observed (Fig. 1). Complete oxidation of iron and its removal from the water column would have left manganese, with a higher electrochemical potential, to buffer oxygen in the surface waters. Precipitation of manganese oxides then occurs. This clearing of iron in the upper layers was probably a transient effect, as banded iron deposition continued for the following ≈400 My. In modern eutrophic lakes, manganese oxidation is vastly accelerated by bacteria, and the deposition of aqueous manganese is directly coupled with the release of O_2 from cyanobacterial blooms (41), conditions that are similar to those inferred for the deposition of BIFs (42, 43). These postsnowball oceanic conditions closely match models for the deposition of both early and late Proterozoic sedimentary manganese formations (24, 25, 27). The Fe and Mn that accumulated in the global ocean would have been sufficient to form deposits like the basal 50 m of the Hotazel formation over an area of 10^6–10^7 km², a significant fraction of the present total area of continental shelves (3×10^7 km²). Deposition in deeper, anoxic waters would have been inhibited by biochemical recycling (reduction of the Fe and Mn oxides). About ≈10^{19} mol (0.06 bar) of CO_2 would have to have been photosynthetically fixed to release enough molecular oxygen to precipitate this quantity of metal. Much of the remaining CO_2 could have been precipitated as carbonates (limestone or dolomite) as the postsnowball atmosphere came to equilibrium with the ocean (10).

The lack of organic material in BIFs has been used to argue against biological mechanisms of oxidation (42). In the modern oceans, however, most organic matter is transported to the
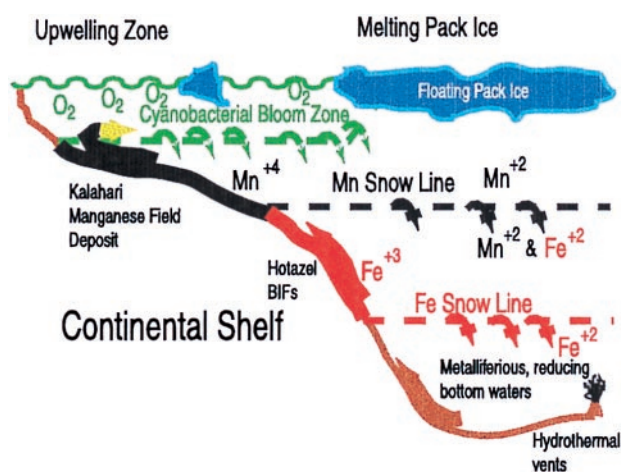

Fig. 3. Schematic setting for deposition of the Kalahari Manganese Field in a postsnowball environment. Upon initial melting, the cyanobacterial bloom exposes the anoxic, metalliferous waters to free O_2 in the euphotic zone. Initially, both Mn^{+4} and Fe^{+3} precipitate out and settle gravitationally. However, when the Mn^{+4} sinks to waters still containing Fe^{+2} in solution, the manganese will be re-reduced to the soluble Mn^{+2}, generating more Fe^{+3} precipitate. (This reaction may be biologically mediated.) Eventually, the iron is stripped out of the surface zone, forming the Mn ''snow line'' as indicated. Continued upwelling of waters on the edge of the platform should increase the Mn concentration, allowing Mn precipitates to collect on the platform, producing the Kalahari manganese ore deposits in the Hotazel Formation. Below the Mn snow line, both Fe^{+2} and Mn^{+2} would be in solution whereas Fe^{+3} minerals are precipitating to form the iron stones. If the bottom waters are reducing enough, there may even be an Fe snow line, below which the Fe^{+3} is reduced and returned to solution. (No sediments from this depth appear to be preserved in the Kalahari.) Small changes in relative sea level could then cause these metal snow lines to move up and down the platform, yielding some of the lateral and temporal variations in the Kalahari manganese field deposits (23).

sediments by fecal pellets from the zooplankton (44). Without this mechanism, organic matter would have been recycled largely within the mixed layer of the surface ocean, and the heavier Fe and Mn precipitates could have settled out separately. This is consistent with isotopic data for carbonate carbon in the Hotazel Formation and the overlying dolomites, which follow a pattern somewhat similar to those reported for Neoproterozoic glaciogenic rocks in Namibia (10). Although marine sediments deposited immediately before the onset of glaciation are not preserved in the Transvaal group, our $\delta^{13}C$ values from the Mn-carbonates in the Hotazel formation (Fig. 1) range from -12 to $-15‰$, those from primary $FeCO_3$ (siderite) in its uppermost units are around $-7‰$, and values from the Mooidraai Dolomite return to typical marine values of about $+0.7‰$. We interpret these data from the Mn-carbonates as indicating a contribution from mantle-derived CO_2 built up in the oceans during the snowball event (which should be in the -5 to $-7‰$ range), with some input from the organic carbon produced during the peak cyanobacterial bloom (and perhaps settling out with the metals) having caused the re-reduction of the Mn^{+4} during diagnesis. Note that we do not see a volcanic $\delta^{13}C$ signature ($\approx -6‰$) in the first postsnowball sediments, as is present in the Neoproterozoic cap carbonates (10). Our postglacial Sr isotopic ratios are also radiogenic ($^{87}Sr/^{86}Sr$ values of 0.704 to 0.705 in the Mn-carbonates, and as high as 0.71 in the Mooidraai Dolomite). This suggests that a significant quantity of glacial dust from the continents was deposited on the floating pack ice, complimenting a significant contribution of riverine water from postglacial greenhouse-induced weathering on the continents (13).

Kirschvink *et al.*

Paleobiological Implications. Hoffman *et al.* (10) argue that the smaller Neoproterozoic glaciations may have triggered the apparent evolution of metazoan life observed in the fossil record. In contrast, the early Proterozoic record consists strictly of stromatolites and single-cell microfossils. Evolution in these organisms is primarily biochemical, rather than morphological, and difficult to constrain by the direct fossil record. We propose that the appearance of the Kalahari manganese field in the geologic record provides insight into biologically mediated geochemistry during the Paleoproterozoic and, by inference, the evolution of important metabolic pathways. First, oxidation of the Mn in the Kalahari deposit, extrapolated to a large basin or continental shelf setting, required molecular oxygen equivalent to several tenths of a bar. This is in contrast to the Fe in Archean BIFs, for which several oxidizing mechanisms have been proposed (45, 46), or early stromatolites, which could have been produced by either anoxic or oxic photosynthetic organisms (47). Although abiotic photochemistry might produce trace amounts of oxygen on the early Earth, only oxygenic photosynthesis by cyanobacteria could plausibly produce this much oxygen in a geologically short period of time. The Mn deposit thus places the origin of oxygenic photosystem II before 2.4 Ga, consistent with the identification of cyanobacterial biomarkers in 2.5- to 2.7-Ga rocks (40). Second, the uncatalyzed oxidation of Mn is extremely slow, and, even in modern, highly oxidized environments, it proceeds exclusively via bacterial mediation at rates accelerated by several orders of magnitude (41). The massive deposition of Mn suggests high bacterial cell densities, and under highly oxidizing conditions this implies that bacteria (particularly cyanobacteria) had developed mechanisms of defense against molecular oxygen and its radical byproducts. The origin of these oxygen-related pathways has been argued on a phylogenetic basis (48). To our knowledge this is the oldest physical evidence for this adaptation.

Finally, we speculate that the predicted severity of climate and geochemical change during the snowball event and its aftermath may have forced enormous biological adaptation and left recognizable signatures in the phylogenies of extant organisms and their genes. The timing of the appearance of the first oxidizing environments is unknown. Several lines of evidence support significant levels of atmospheric oxygen by 2.2 Ga (29). However, oxidizing "microenvironments" created by oxygenic photosynthesis may have arisen much earlier. The manganese deposition event described here records the oldest known appearance of large-scale oxidized environments on the Earth, occurring when the bulk of the world's oceans were of reducing character (49). The introduction of significant amounts of molecular oxygen, regardless of when it first occurred, differentiated ecological niches by oxidation state and hence the concentration of soluble Fe^{2+} and Mn^{2+}. Specifically, oxidation and precipitation of manganese would occur only after complete depletion of ferrous iron.

Iron and manganese are metal cofactors in many important enzymes, and environments with extreme differences in their concentrations would select for organisms and enzymes adapted to those circumstances. Evolutionary pressure would select between metalloenzymes on the basis of their metal content. Multiple forms of an enzyme, each with a metal content optimized for a particular environment, could arise through the processes of gene duplication or speciation. The common ancestry of these different isozymes can be recognized by comparing their amino acid sequences. In principle, the construction of a phylogenetic tree based on the inferred homologies provides information about the sequence divergence between the different enzyme isoforms relative to the divergence between the same isoform found in different groups of organisms. We emphasize that such a tree reflects the evolution of a single molecule, not necessarily the evolution of organisms (as trees constructed from
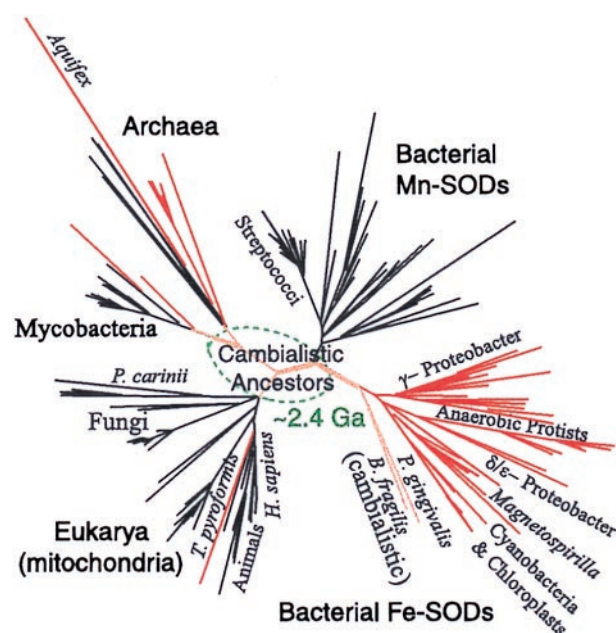

Fig. 4. Unrooted phylogenetic tree constructed from the alignment of 214 Fe/Mn super oxide dismutase (SOD) amino acid sequences. The branches are color coded as Fe-SODs (red), cambialistic (Fe or Mn) SODs (orange), and Mn-SODs (black). The portion of the tree estimated to be older than the Paleoproterozoic snowball Earth event at 2.4 Ga is located inside the dotted oval, and hypothesized to be cambialistic. The National Center for Biotechnology Information protein and nucleotide database Entrez search tool was used to obtain 206 sequences; the sequences of two *Magnetospirillum* strains, MS-1 (ATCC 31632) and AMB-1 (ATCC 700264) and a *Magnetovibrio* strain MV-1 (gift of D. Dean, Virginia Tech.) were obtained from genomic DNA by PCR using the degenerate primers 5″-AIGTAGTAIGCITGITCCCA-3″ and 5″-AIACIATGGAAATCCACCA-3″. Additional sequence for MV-1 was obtained by PCR using 5″-AAGCACCACGIGICCTACGT-3″ together with the second primer given above and for MS-1 by using the PCR product to probe a small insert *Eco*RI library of MS-1 DNA. An *Aquifex* sequence was obtained from ref. 64. The sequences were trimmed to a region similar to that chosen by Smith and Doolitle (53) of about 136 aa (in human) from just N-ward of the first His metal ligand to just C-ward of the Asp ligand. Multiple sequence alignment was performed by CLUSTAL W (65) using the BLOSUM62 matrix (66) and was manually inspected by location of the extremely conserved metal ligand residues (His-His-Asp-His). The tree shown is heuristically generated by CLUSTAL W, and branch lengths are corrected for multiple substitutions. Although the precise position of many species is uncertain, particularly those with long branch lengths, the basic branching topology agrees with parsimony trees generated by using the PHYLIP package (67) and is strongly supported by bootstrap analysis.

ribosomal RNA may). To the extent that the degree of sequence divergence between two sequences represents elapsed time since a common ancestor, this phylogeny could provide information on the relative timing of major evolutionary events.

The iron/manganese superoxide dismutase [Fe/Mn-superoxide dismutase (SOD)] enzyme, which catalyzes reduction of O_2^- to H_2O_2 or O_2, is particularly well suited for such an investigation. This highly conserved enzyme, found in all three domains of life (Eukarya, Archaea, and Bacteria), exists in two distinct but related forms distinguished by metal cofactor preference. Organisms have presumably evolved or acquired Fe or Mn SODs as required by their lifestyle: Because the metal cofactors are engaged in the transfer of electrons to or from the O_2^- radical, the redox state of the environment may exert selective pressure on the use of the Fe or Mn form not only on the basis of their availability but on their different electrochemical potentials as well. Some facultative organisms, such as *Escherichia coli*, use both forms. The amino acid sequence similarity

and nearly identical tertiary structures of Fe and Mn SODs establish their common evolutionary origin (50–52).

A phylogenetic tree constructed from highly conserved portions of 214 unique SOD sequences (Fig. 4) confirms and expands on the previous work of Smith and Doolittle (53) and Brown and Doolittle (54). The three domains of life inferred from ribosomal RNA (55) are represented in this protein tree. The bacterial forms of SOD are divided into two clades correlated with enzyme metal content, a division that is not simply a mirror of the divergences of major lineages as defined by ribosomal RNA phylogenies. (Poorly defined divergences by cofactor preference also appear in the Archaea whereas only a single Fe SOD, that of *Tetrahymena pyroformis*, is known among the higher Eukaryota.) The phylogeny of the SOD enzyme suggests that the bacterial Mn and Fe isoforms diverged after the domains of the Archea and Bacteria separated from a common ancestor perhaps 3–4 Ga (56, 57). The cofactor preference of the ancestral enzyme is unknown, but before the appearance of oxidizing environments there would have been only slight environmental pressure for selection of the more plentiful Fe in lieu of Mn, and the enzyme may have used both metals (cambialistic). The appearance of the cambialistic enzymes in two cytophagales (*Bacteroides fragilis* and *Porphyromonas gingivalis*) close to the Fe-Mn node supports this hypothesis.

Further interpretation of the phylogenetic tree can only be highly speculative, and the detailed evolution of the SOD enzyme is probably quite complex (58). The metal cofactors of many SODs in the literature were identified on the basis of the amino acids present at a few key sites in the protein, rather than spectroscopy or chemical assay. This identification may be susceptible to a small number of mutations that result in an apparent change of phenotype. Protein phylogenies can be affected by horizontal gene transfer between distant groups of organisms. In the case of the Eukarya, this gene transfer appears to have been widespread: The eukaryotic sequences are distributed between the bacterial Fe SODs (euglenozoa, alvolae, and the parabasalidae), the cyanobacteria (chloroplast SODs), and a monophyletic group of mitochondria-targeted sequences that diverge from the Archaea. A single *Chlomydomonas* sequence appears with the bacterial Mn SODs, and the SOD from *Pneumocystis carinii*, an opportunistic parasite with molecular features of both fungi and protozoa (59), branches at an ill-determined location between the Archaea and the Eukarya. As noted in previous work, the phylogeny of the mitochondrial sequences is paradoxical because they do not branch with the lineage of a plausible ancestral symbiont (α-proteobacteria) as the chloroplast sequences do. Ironically, the sequenced SODs of protists, with the exception of the alveolata *T. pyriformis*, appear with the Fe SODs of the α-proteobacteria. It would appear that this massive gene transfer, which may have been associated with endosymbiosis, occurred subsequent to the metal divergence event. The oldest fossil Eukaryote (*Grypania*), interpreted to possess mitochondria on the basis of morphology, are found in shales from the 1.9- to 2.1-Ga Negaunee Iron Formation (60). Biomarkers indicative of eukaryotic organisms have been found in 2.5- to 2.7-Ga rocks (40), but the complexity of the source organisms is unknown.

We emphasize that our phylogenetic analysis of the SOD enzyme describes one potential evolutionary consequence of a change in the redox state of the Earth's surface and does not provide independent evidence for the snowball event. However, if our snowball model of the Paleoproterozoic Kalahari Manganese deposition is correct, we have identified an extreme and rapid change in climate and geochemistry of a magnitude dwarfing later catastrophes such as the Cretaceous-Tertiary impact. The persistence of globally subfreezing temperatures, the isolation of the ocean from sunlight, the interruption of the hydrological cycle, and the absence of liquid water on continents for tens of millions of years would have presented microorganisms with few viable options for habitable ecosystems. Polar cryptoendolithic communities, like those that exist today in the dry valleys of Antarctica, require a short but critical summer period of temperatures above freezing (61). Extreme selection and rapid biological adaptation may have produced a "bottleneck" in genomes through which we have only a narrow and biased view of Archean life. A similar hypothesis has invoked a hot, heavily impacted early Earth to explain the preferential appearance of hyperthermophilic organisms near the location of the last common ancestor of the three kingdoms on 16s RNA phylogenetic trees (62, 63). We note that, during a long snowball state, hydrothermal springs may have been one of the few places on Earth where liquid water was continuously maintained in the presence of sunlight.

1. Hambrey, M. J. & Harland, W. B. (1981) *Earth's PrePleistocene Glacial Record* (Cambridge Univ. Press, Cambridge, U.K.).
2. Chumakov, N. M. & Elston, D. P. (1989) *Episodes* **12**, 115–119.
3. Embleton, B. J. J. & Williams, G. E. (1986) *Earth Planet. Sci. Lett.* **79**, 419–430.
4. Schmidt, P. W., Williams, G. E. & Embleton, B. J. J. (1991) *Earth Planet. Sci. Lett.* **105**, 355–367.
5. Schmidt, P. W. & Williams, G. E. (1995) *Earth Planet. Sci. Lett.* **134**, 107–124.
6. Evans, D. A., Beukes, N. J. & Kirschvink, J. L. (1997) *Nature (London)* **386**, 262–266.
7. Williams, G. E. & Schmidt, P. W. (1997) *Earth Planet. Sci. Lett.* **153**, 157–169.
8. Caldeira, K. & Kasting, J. F. (1992) *Nature (London)* **359**, 226–228.
9. Wetherald, R. T. & Manabe, S. (1975) *J. Atmos. Sci.* **32**, 2044–2059.
10. Hoffman, P. F., Kaufman, A. J., Halverson, G. P. & Schrag, D. P. (1998) *Science* **281**, 1342–1346.
11. Hoffman, P. F., Schrag, D. P., Halverson, G. P. & Kaufman, J. A. (1998) *Science* **282**, 1645–1646.
12. Hoffman, P. F. & Maloof, A. C. (1999) *Nature (London)* **397**, 384.
13. Hoffman, P. F. (1999) *Nature (London)* **400**, 708.
14. Kirschvink, J. L. (1992) in *The Proterozoic Biosphere: A Multidisciplinary Study*, eds. Schopf, J. W., Klein, C. & Des Maris, D. (Cambridge Univ. Press, Cambridge, U.K.), pp. 51–52.
15. Tsikos, H. & Moore, J. M. (1998) *S. Afr. J. Earth Geol.* **101**, 287–290.
16. Button, A. (1974) *Trans. Geol. Soc. S. Afr.* **77(2)**, 99–104.
17. Bau, M., Romer, R. L., Lueders, V. & Beukes, N. J. *Earth Planet. Sci. Lett.*, in press.
18. Romer, R. L. & Bau, M. (1998) *Chin. Sci. Bull.* **43**, 109.
19. Cornell, D. H., Schuette, S. S. & Eglington, B. L. (1996) *Precambrian Res.* **79**, 101–123.
20. Hofmann, C., Courtillot, V., Feraud, G., Rochette, P., Yirgu, G., Ketefo, E. & Pik, R. (1997) *Nature (London)* **389**, 838–841.
21. Roy, S. (1981) *Manganese Deposits* (Academic, London).
22. Gutzmer, J., Beukes, N. J. & Yeh, H. W. (1997) *S. Afr. J. Geol.* **100**, 53–71.
23. Cairncross, B., Beukes, N. J. & Gutzmer, J. (1997) *The Manganese Adventure: The South African Manganese Fields* (Associated Ore & Metal Corporation, Johannesburg, South Africa).
24. Buehn, B., Stanistreet, I. G. & Okrusch, M. (1992) *Econ. Geol.* **87**, 1393–1411.
25. Urban, H., Stribrny, B. & Lippolt, H. J. (1992) *Econ. Geol.* **87**, 1375–1392.
26. Trompette, R., De Alvarenga, C. J. S. & Walde, D. (1998) *J. S. Am. Earth Sci.* **11**, 587–597.
27. Schissel, D. & Aro, P. (1992) *Econ. Geol.* **87**, 1367–1374.
28. Klein, C., Beukes, N. J. & Schopf, J. W. (1987) *Precambrian Res.* **36**, 81–94.
29. Rye, R. & Holland, H. D. (1998) *Am. J. Sci.* **298**, 621–672.
30. Veizer, J. (1994) *Geochemistry of Carbonates and Realted Topics: Database* (Ruhr Univ. Press, Bochum, Germany).
31. Swart, Q. (1999) Master's thesis (Rand Afrikaans Univ., Johannesburg).
32. Gutzmer, J. & Beukes, N. J. (1996) *Econ. Geol.* **91**, 1435–1454.
33. Williams, S. N., Schaefer, S. J., Calvache, M. L. & Lopez, D. (1992) *Geochim. Cosmochim. Acta* **56**, 1765–1770.
34. Gough, D. O. (1981) *Solar Phys.* **74**, 21–34.
35. Forget, F. & Pierrehumbert, R. T. (1997) *Science* **278**, 1273–1276.
36. Yung, Y. L., Nair, H. & Gerstell, M. F. (1997) *Icarus* **130**, 222–224.
37. Andreae, M. O. (1996) *Nature (London)* **380**, 389–390.

38. Elderfield, H. & Schultz, A. (1996) *Annu. Rev. Earth Planet. Sci.* **24,** 191–224.
39. Coale, K. H., Johnson, K. S., Fitzwater, S. E., Gordon, R. M., Tanner, S., Chavz, F. P., Ferioli, L., Sakamoto, C., Rogers, P., Millero, F., *et al.* (1996) *Nature (London)* **383,** 495–501.
40. Brocks, J. J., Logan, G. A., Buick, R. & Summons, R. E. (1999) *Science* **285,** 1033–1036.
41. Aguilar, C. & Nealson, K. H. (1998) *J. Great Lakes Res.* **24,** 93–104.
42. Beukes, N. J. & Klein, C. (1992) in *The Proterozoic Biosphere: A Multidisciplinary Study,* eds. Schopf, J. W. & Klein, C. (Cambridge Univ. Press, New York), pp. 147–152.
43. Klein, C. & Beukes, N. J. (1993) *Econ. Geol.* **88,** 542–565.
44. Paffenhofer, G.-A. & Knowles, S. C. (1979) *J. Mar. Res.* **37,** 35–49.
45. Canfield, D. E. (1998) *Nature (London)* **396,** 450–453.
46. Ehrenreich, A. & Widdel, F. (1994) *Appl. Environ. Microbiol.* **60,** 4517–4526.
47. Schopf, J. W. & Klein, C. (1992) *The Proterozoic Biosphere: A Multidisciplinary Study* (Cambridge Univ. Press, Cambridge, U.K.).
48. Castresana, J. & Saraste, M. (1995) *Trends Biochem. Sci.* **20,** 443–448.
49. Kasting, J. F. (1993) *Science* **259,** 920–926.
50. Parker, M. W., Blake, C. C. F., Barra, D., Bossa, F., Schinina, M. E., Bannister, W. H. & Bannister, J. V. (1987) *Protein Eng.* **1,** 393–397.
51. Carlioz, A., Ludwig, M. L., Stallings, W. C., Fee, J. A., Steinman, H. M. & Touati, D. (1988) *J. Biol. Chem.* **263,** 1555–1562.
52. Grace, S. C. (1990) *Life Sci.* **47,** 1875–1886.
53. Smith, M. W. & Doolittle, R. F. (1992) *J. Mol. Evol.* **34,** 175–184.
54. Brown, J. R. & Doolittle, W. F. (1997) *Microbiol. Mol. Biol. Rev.* **61,** 456–502.
55. Woese, C. R. (1987) *Microbiol. Rev.* **51,** 221–271.
56. Feng, D. F., Cho, G. & Doolittle, R. F. (1997) *Proc. Natl. Acad. Sci. USA* **94,** 13028–13033.
57. Iwabe, N., Kuma, K., Hasegawa, M., Osawa, S. & Miyata, T. (1989) *Proc. Natl. Acad. Sci. USA* **86,** 9355–9359.
58. Phalgun, J. & Dennis, P. P. (1993) *J. Bacteriol.* **175,** 1572–1579.
59. Edman, J. C., Kovacs, J. A., Masur, H., Santi, D. V., Elwood, H. J. & Sogin, M. L. (1988) *Nature (London)* **334,** 519–522.
60. Han, T. M. & Runnegar, B. (1992) *Science* **257,** 232–235.
61. Friedmann, E. I., Kappen, L., Meyer, M. A. & Nienow, J. A. (1993) *Microb. Ecol.* **25,** 51–69.
62. Maher, K. A. & Stevenson, D. J. (1988) *Nature (London)* **331,** 612–614.
63. Miller, S. L. & Lazcano, A. (1995) *J. Mol. Evol.* **41,** 689–692.
64. Lim, J. H., Yu, Y. G., Choi, I. G., Ryu, J. R., Ahn, B. Y., Kim, S. H. & Han, Y. S. (1997) *FEBS Lett.* **406,** 142–146.
65. Thompson, J. D., Higgins, D. G. & Gibson, T. J. (1994) *Nucleic Acids Res.* **22,** 4673–4680.
66. Henikoff, S. & Henikoff, J. G. (1992) *Proc. Natl. Acad. Sci. USA* **89,** 10915–10919.
67. Felsenstein, J. (1996) in *Computer Methods For Macromolecular Sequence Analysis,* ed. Doolittle, R. (Academic, San Diego), vol. 266, pp. 418–427.

EVOLUTION

GEOLOGY

SPECIAL FEATURE